

Scintillation Response of Activated Inorganic Crystals to Various Charged Particles

R. B. MURRAY AND A. MEYER
Oak Ridge National Laboratory,* Oak Ridge, Tennessee
(Received December 5, 1960)

Experimental studies of the response of activated ionic crystals such as NaI(Tl) and CsI(Tl) to heavy charged particles indicate decreasing scintillation efficiency with increasing particle mass, and a nonlinearity in pulse height versus energy for heavier particles. Recent experiments indicate that the scintillation efficiency to electrons, however, is less than that to protons. In an attempt to account for these effects, this paper presents a calculation based on a model of the process of energy transfer from the incoming particle to the activator sites. In this model, the energy carriers are taken to be excitons resulting from recombination of electron-hole pairs in the wake of the particle. The migration of carriers to activator sites is described by a one-velocity diffusion equation in which the density of unoccupied activator sites, N_a , is a function

of space and time. The diffusion equation is coupled with a second differential equation describing the time dependence of N_a . The solution to these equations indicates that the depletion of available activator sites by a particle with high dE/dx can account for observed saturation effects. This model further contains the activator concentration as a parameter, and permits a prediction of scintillation efficiency as a function of both dE/dx and concentration. The low scintillation efficiency to electrons is predicted as a consequence of the smaller recombination probability for particles of very low dE/dx . Finally, for a low- dE/dx particle in a crystal of 0.1-mole-percent activator concentration the diffusion length of energy carriers is found to be of order 20 Å.

I. INTRODUCTION

THE scintillation response of activated inorganic crystals to various charged particles has been the subject of numerous experimental studies.¹ Most of the interest in this subject has been focused on activated alkali iodides, as these crystals are most commonly used in scintillation counting and spectrometry. All five alkali iodides (LiI, NaI, KI, RbI, CsI) are known to be reasonably efficient scintillators at room temperature when activated by a heavy-element impurity with a concentration of order 10^{-1} mole percent. LiI is typically activated with Eu for highest scintillation efficiency, while the remaining four alkali iodides are usually activated with Tl. In reviewing the experimental results describing the response to charged particles, several general features are observed in the various crystals: (a) The pulse height versus energy relationship is nearly linear over a wide energy range for electrons, protons, and deuterons; (b) the pulse height versus energy curve is distinctly nonlinear for alphas and heavier particles of energy several Mev, tending to curve away from the energy axis; (c) the pulse height per unit energy loss decreases with increasing particle mass in going from protons to alphas, carbon ions, etc.; (d) the pulse height per unit energy loss for electrons is less than that for protons in at least four of the activated alkali iodides.²⁻⁴

Although the above items seem to be well documented and have been the subject of qualitative discussion, there has been rather little effort to interpret these effects in terms of the details of the scintillation process. Items (b) and (c) are frequently attributed to "saturation

of the luminescence centers," referring to a depletion of available activator sites by a particle with high dE/dx . To the authors' knowledge, however, this concept has not been critically examined. It is the object of this paper to describe the events leading to a scintillation pulse by means of a simple, phenomenological model, in an attempt to account for the above effects. In particular, we wish to examine the saturation mechanism to determine whether it may reasonably explain the experimental data on scintillation efficiency as a function of dE/dx of the incoming particle and as a function of the activator concentration of the crystal.

It is appropriate to note at this point that organic scintillators exhibit features qualitatively similar to items (b) and (c) above. Birks⁵ has proposed a function describing the pulse height versus energy relationship which seems to be in good agreement with experiment; this function is derived from considerations of radiation damage along the path of an ionizing particle in an organic solid. The rather good agreement with experiment of this and similar functions⁶ need not imply, however, that such a relationship should describe the situation in *inorganic* crystals. The scintillation processes in organic and activated inorganic crystals are basically different, and a description of one should not necessarily provide a description of the other. In particular, the Birks function predicts a considerably greater pulse height per Mev for electrons than for protons, in distinct contrast with experimental results from inorganic crystals.

II. REVIEW OF EXPERIMENTAL RESULTS

In the present work we will deal in large part with the relationship between scintillation efficiency and the

* Operated by Union Carbide Corporation for the U. S. Atomic Energy Commission.

¹ For a recent bibliography of various papers on this subject, see W. E. Mott and R. B. Sutton, *Encyclopedia of Physics*, edited by S. Flügge (Springer-Verlag, Berlin, 1958), Vol. 45, p. 86.

² P. Kienle and R. E. Segel, *Phys. Rev.* **113**, 909 (1959).

³ T. R. Ophel, *Nuclear Instr.* **3**, 45 (1958).

⁴ R. S. Storey, W. Jack, and A. Ward, *Proc. Phys. Soc. (London)* **72**, 1 (1958).

⁵ J. B. Birks, *Scintillation Counters* (McGraw-Hill Book Company, Inc., New York, 1953).

⁶ For a summary, see F. D. Brooks, Chapter in: *Progress in Nuclear Physics*, edited by O. R. Frisch (Pergamon Press, New York, 1956), Vol. 5, p. 252.

stopping power of the particle in a particular alkali iodide. *Scintillation efficiency* is here defined as dL/dE , the slope of a pulse height versus energy curve; stopping power is defined as $-dE/dx$, the negative differential energy loss per unit path length. In particular, we will be concerned with the shape of the dL/dE versus dE/dx curve. The use of dE/dx as a parameter is an attempt to reduce the response to different particles to a common denominator, i.e., a parameter by means of which one curve will describe the response to all particles. The scintillation efficiency dL/dE is, of course, a differential quantity describing the number of photons emitted per unit energy loss for a particle of energy E . It is to be emphasized that both the scintillation efficiency and stopping power are functions of the particle energy and are uniquely defined for a specified particle of energy E in a particular crystal. It may also be noted that dL/dE is generally quite different from L/E , as the latter quantity represents an average over the entire path of the particle.

In order to compare the present work with experiment, it would be most desirable to have available pulse height versus energy curves for many particles, spanning a wide range in energy, on one particular crystal of, say NaI(Tl). Unfortunately, such information is not available as the result of a single experiment. It is thus necessary to refer to numerous experiments and attempt to synthesize the available information into a coherent picture. Since most of the experimental information refers to NaI(Tl), KI(Tl), and CsI(Tl), we will summarize the results for these materials only. The scintillation efficiency dL/dE can be obtained from tables or figures in the various papers; the stopping power must, however, be calculated as a function of energy for a particular particle in NaI(Tl), KI(Tl), or CsI(Tl).

The calculation of stopping power for protons and alpha particles in these three alkali iodides was carried out with reference to Whaling's recent summary⁷ of the stopping cross section of various elements for elementary particles. The stopping cross section for protons in each of the four elements, Na, K, Cs, and I was calculated with reference to experimental values in neighboring elements using a linear interpolation in atomic number. The stopping cross section for protons in each of the four elements at 20 Mev was calculated with the parameters given by Whaling (his Table I), and using the same interpolation scheme as above. Knowing the stopping cross section for protons in each of these elements as a function of energy, the corresponding quantity for deuterons and alphas was calculated directly using the prescriptions of reference 7. The stopping cross sections of the elements were added to obtain that for the compound, and divided by the mass of the alkali iodide molecule to obtain stopping power in kev-cm²/mg. The results for all three crystals are pre-

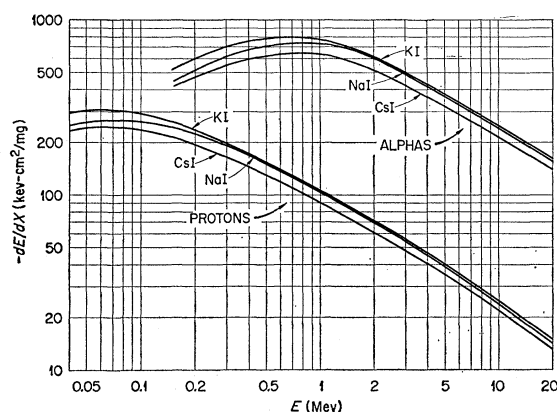


Fig. 1. Calculated differential energy loss as a function of energy for protons and alphas in KI, NaI, and CsI.

sented in Fig. 1. In order to avoid confusion in the figure the deuteron curves are not shown; they may be readily obtained from the proton curves in the usual manner.⁷

A similar calculation for NaI has been given previously by Eby and Jentschke.⁸ Their results are in agreement with those presented here for both protons and alphas for energies above 4 or 5 Mev. At lower energies, however, their curves are below those of Fig. 1, the deviation amounting to $\sim 30\%$ below 1 Mev. The source of this discrepancy undoubtedly arises from the different values of dE/dx for various elements used in the two calculations. For example, the dE/dx values for alpha particles with energies less than 2 Mev were calculated by Eby and Jentschke on the basis of measured stopping powers of different substances relative to air reported in the 1936 Landolt-Börnstein tables.⁹

The stopping power of NaI for electrons in the interval 0.01 to 1.2 Mev was taken directly from a calculation by Nelms¹⁰ and includes correction for the density effect. Above 1.2 Mev, up to energies of a few Mev, it is assumed that dE/dx for electrons is constant; this approximation is quite good for present purposes. The stopping powers of CsI and KI to electrons are not needed accurately for this work; accordingly, they have been taken as equal to that of NaI, expressed in kev-cm²/mg. In the energy region considered here, energy loss of electrons to bremsstrahlung amounts to a few percent at most and need not be considered further.

The calculation of dE/dx for heavier nuclei (C^{12} , N^{14} , etc.) in the alkali iodides was carried out with reference to recent studies¹¹ which permit a determination of the average on a particle as a function of its velocity during

⁸ F. S. Eby and W. K. Jentschke, Phys. Rev. **96**, 911 (1954).

⁹ H. H. Landolt and R. Börnstein, *Physikalisch-Chemische Tabellen* (Verlag Julius-Springer, Berlin, 1936), 5th ed., third supplementary volume, second part.

¹⁰ Ann T. Nelms, National Bureau of Standards Circular No. 577 Supplement (Superintendent of Documents, U. S. Government Printing Office, Washington, D. C., 1958).

¹¹ A. Papineau, Compt. rend. **242**, 2933 (1956); also H. H. Heckman, B. L. Perkins, W. G. Simon, F. M. Smith, and W. H. Barkas, Phys. Rev. **117**, 544 (1960).

⁷ W. Whaling, *Encyclopedia of Physics*, edited by S. Flügge (Springer-Verlag, Berlin, 1958), Vol. 34, p. 193.

the slowing-down process. In so doing, it is assumed that Z_{eff} as a function of velocity is essentially independent of the stopping medium, and that the curves¹¹ of Z_{eff}/Z versus β/Z^2 may be applied to the materials of interest here. Knowing Z_{eff} , the stopping power of, say, N^{14} in NaI is then calculated as

$$\left(\frac{dE}{dx}\right)_{\text{N}^{14}} = \left(\frac{Z_{\text{eff}}}{Z_p}\right)^2 \left(\frac{dE}{dx}\right)_p, \quad (1)$$

where $(dE/dx)_p$ refers to the stopping power of NaI to a proton of the same velocity as the N^{14} ion, and Z_p represents the effective proton charge at that velocity. The effective proton charge is taken as unity above 400 kev. Below 400 kev, Z_p is calculated on the basis of measured electron capture cross sections as a function of proton velocity in various media.¹² The results of these calculations of dE/dx versus E for a heavy particle give a function with a broad maximum in the region 1 to 15 Mev, and are comparable with the results of Newman and Steigert.¹³

Finally, the stopping power of CsI to fission fragments is taken directly from the work of Fulmer.¹⁴ For present purposes it is assumed to be the same in other alkali iodides.

Combining the pulse height versus energy data from various experiments with the above calculations of dE/dx versus energy, it is now possible to illustrate the general features of the scintillation efficiency as a function of stopping power. Such a summary involves, of course, the results of various experiments using different crystals and performed with various charged particles. Clearly, this procedure is subject to considerable quantitative uncertainty; it is, nevertheless, of interest to summarize the data in this way as the over-all features of the curve may be demonstrated even with the uncertainties which are involved.

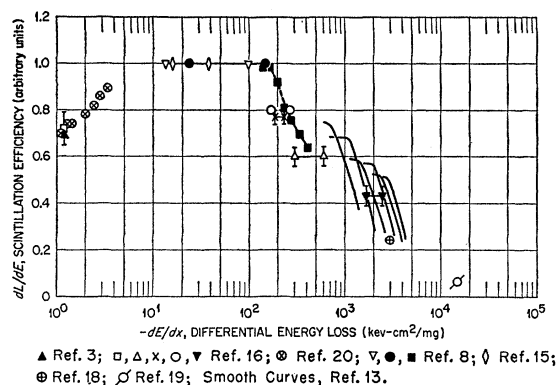


FIG. 2. Scintillation efficiency as a function of dE/dx for various particles in NaI(Tl).

¹² A. Berthelot, *Rayonnements de Particules Atomiques, Electrons et Photons* (Masson et Cie, Paris, 1956), Chap. 4.

¹³ E. Newman and F. E. Steigert, *Phys. Rev.* **118**, 1575 (1960).

¹⁴ C. B. Fulmer, *Phys. Rev.* **108**, 1113 (1957).

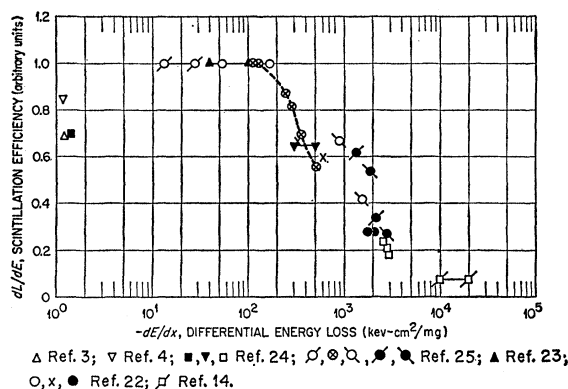


FIG. 3. Scintillation efficiency as a function of dE/dx for various particles in CsI(Tl).

A summary of experimental evidence for NaI(Tl) is given in Fig. 2, where the scintillation efficiency for protons of energy several Mev and greater has been normalized to unity. (There is always an arbitrary normalization factor which must be assigned, since experiments give only *relative* pulse heights.) Experimental data for protons, deuterons, alphas, various heavy ions (B^{10} through Na^{23}), and fission fragments are taken from various sources.^{8,13,15-19} The response of NaI(Tl) to electrons (from gamma rays) relative to heavier particles is taken from two studies.^{3,16} The scintillation efficiency to electrons of different energy, in Fig. 2, is based on the gamma-ray experiments of Engelkemeier and those of Managan.²⁰ The electron data points in Fig. 2 were calculated as dL/dE for *electrons*, but were based on the experimental gamma-ray response curves.²⁰ This calculation²¹ takes into account the multiple nature of the gamma-ray interaction with electrons of the crystal through photoelectric, Compton, and pair-production events. The electron data points of Fig. 2 were normalized for high-energy electrons (~ 1 Mev) to 0.7, the average of the points from references 3 and 16.

Turning next to CsI(Tl) the scintillation efficiency to various charged particles is illustrated in Fig. 3, again with the Mev proton data normalized to 1.0. The response to charged particles ranging from protons to fission fragments is taken from various papers.^{14,22-25} A comparison between scintillation efficiency to protons

¹⁵ J. G. Likely and W. Franzen, *Phys. Rev.* **87**, 666 (1952).

¹⁶ S. K. Allison and H. Casson, *Phys. Rev.* **90**, 880 (1953).

¹⁷ J. E. Brolley and F. L. Ribe, *Phys. Rev.* **98**, 1112 (1955).

¹⁸ E. N. Shipley, G. E. Owen, and L. Madansky, *Rev. Sci. Instr.* **30**, 604 (1959).

¹⁹ J. C. D. Milton and J. S. Fraser, *Phys. Rev.* **96**, 1508 (1954).

²⁰ See, *Applied Gamma-Ray Spectrometry*, edited by C. E. Crouthamel (Pergamon Press, New York, 1960), Chap. 2.

²¹ This work has been reported in Oak Ridge National Laboratory Report 3016, 1960, and will be published elsewhere.

²² S. Bashkin, R. R. Carlson, R. A. Douglas, and J. A. Jacobs, *Phys. Rev.* **109**, 434 (1958).

²³ A. Galonsky, C. H. Johnson, and C. D. Moak, *Rev. Sci. Instr.* **27**, 58 (1956).

²⁴ M. L. Halbert, *Phys. Rev.* **107**, 647 (1957).

²⁵ A. R. Quinton, C. E. Anderson, and W. J. Knox, *Phys. Rev.* **115**, 886 (1959).

and electrons (from gamma rays) is available from two studies, that of Ophel³ and that of Storey *et al.*⁴ A further comparison between the response to electrons and heavier charged particles is obtained from the work of Halbert.²⁴ Normalizing Halbert's alpha data to those of Bashkin *et al.*,²² we obtain an electron scintillation efficiency of 0.7, in agreement with Ophel.

In the final case of KI(Tl), the experimental data show the same general trend as in Figs. 2 and 3, and need not be plotted here. We note the experiments of Link and Walker²⁶ who examined the response to protons, deuterons, and alphas. Link and Walker plot their results as dL/dE versus dE/dx and find a continuous function for all three particles with a distinct maximum around 100 kev-cm²/mg, essentially in agreement with Figs. 2 and 3. The response to C¹² ions is reported by Burcham²⁷ and to fission fragments by Milton and Fraser.¹⁹ Kienle and Segel² have reported a scintillation efficiency to electrons which is about 0.7 times the proton efficiency. Thus the over-all features of the KI(Tl) response curve are very similar to those of both NaI(Tl) and CsI(Tl).

In summary, the experimental results on these three crystals illustrate very similar behavior. It may be reiterated here that the individual data points on either Fig. 2 or Fig. 3 are subject to a generous uncertainty. There are two obvious factors which may contribute to an error in the normalization of one set of experimental results to another: (1) The Tl concentration of the crystals used in the various experiments is surely not the same, and (2) the clipping time of the scintillation pulse is not the same in all cases. The observed response curves will depend upon both of these factors; in the latter case, a change in decay time with dE/dx of the incoming particle, as observed in CsI(Tl),⁴ will distinctly influence the relative pulse height between different particles unless the clipping time is very long.

In view of the results of the foregoing data summary, it is reasonable to postulate that a single smooth function may be used to describe the scintillation efficiency as a function of the specific energy loss of the incoming particle. It is further postulated that this relation is a common property of the group of Tl-activated alkali iodides and may be expected to describe the behavior of any member of this group. These assumptions constitute the basis of the model to be proposed in the next section. It should be understood that the concept of a single function describing dL/dE versus dE/dx , independent of the nature of the particle, is based on the observed general trend of experimental data over some four decades of dE/dx . This assumption surely applies to the gross behavior of the scintillation efficiency as seen in Figs. 2 and 3. The possibility still exists that dL/dE for two different particles having the same dE/dx is not exactly the same, in which case the

over-all scintillation efficiency versus dE/dx curve will be made up of a series of discontinuous functions, one for each different particle. This type of behavior is suggested by some of the experimental results from heavy ions.^{13,25} The question of the continuous or discontinuous nature of the scintillation efficiency for different charged particles is a very fundamental issue. On the other hand, this possible discontinuous behavior constitutes a kind of "fine structure" on the over-all curve and as such will not be considered further in the present paper.

III. FORMULATION OF MODEL

Previous studies of the luminescence process in Tl-activated alkali halides^{28,29} indicate that the luminescence radiation is emitted in a transition from an excited state to the ground state of a monovalent Tl⁺ ion. The possibility that luminescence radiation occurs as the result of direct excitation of Tl⁺ sites by an incoming charged particle can be immediately ruled out: The Tl concentration is orders of magnitude too low to account for the observed emission intensity. Excitation of the Tl⁺ sites must then occur as the result of an energy transport process from the path of the incident particle to the various impurity centers. In view of the preceding statements, the energy transport must not affect the charge state of the Tl⁺ center and thus must occur via a carrier or carriers whose net charge is zero. There are several conceivable mechanisms of energy transport which may be considered. They include: (1) photon emission by lattice constituents followed by absorption at Tl⁺ sites; (2) independent (binary) diffusion of electrons and holes from the wake of the charged particle followed by capture of both electron and hole, in succession, at the activator site; and (3) single-particle diffusion of closely coupled electron-hole pairs (excitons), followed by capture at a Tl⁺ site. Of these possibilities, item (1) can be reasonably excluded at the outset on the basis of previous experimental work^{30,31} on NaI(Tl) and CsI(Tl). The two remaining processes have been considered by various authors.²⁹⁻³³ The experimental results of Van Sciver²⁹ on the scintillation properties of nonactivated NaI indicated an exciton transport mechanism; the behavior of NaI(Tl) in its response to charged particles was interpreted in terms of a mixture of items (2) and (3). The recent work of Tomura and Kaifu³⁴ on the luminescence of KI(Tl) also

²⁸ F. E. Williams, *Advances in Electronics*, edited by L. Marton (Academic Press, Inc., New York, 1953), Vol. 5, p. 137.

²⁹ W. J. Van Sciver, IRE Trans. on Nuclear Sci. NS-3, 39 (1956).

³⁰ W. J. Van Sciver, in *Nuclear Electronics* (Proceedings of the International Symposium on Nuclear Electronics, Paris, 1958) (International Atomic Energy Agency, Vienna, 1958), p. 37.

³¹ E. K. Zavoiskii and G. E. Smolkin, Soviet Phys.—Doklady 1, 652 (1956).

³² I. K. Pliavin, Optics and Spectroscopy 7, 41 (1959).

³³ H. Enz and J. Rossel, Helv. Phys. Acta 31, 25 (1958).

³⁴ M. Tomura and Y. Kaifu, J. Phys. Soc. Japan 15, 1295 (1960); also Suppl. Progr. Theoret. Phys. (Kyoto) No. 12, 141 (1959).

²⁶ W. T. Link and D. Walker, Proc. Phys. Soc. (London) A66, 767 (1953).

²⁷ W. E. Burcham, Proc. Phys. Soc. (London) A70, 309 (1957).

indicates the role of exciton transfer. Thus there is experimental evidence indicating that exciton transport can contribute to the scintillation process. This does not, however, eliminate the possibility of a contribution from binary diffusion of electrons and holes, item (2).

The principal distinction between mechanisms (2) and (3) has to do with the strength of coupling between electron and hole: Item (2) implies no coupling between electron and hole, whereas a strictly single-particle diffusion, item (3), implies such strong coupling between electron and hole that they are never separated. Experimental observations on alkali halides in general indicate that the electron and hole are indeed strongly coupled, but not necessarily to the extent implied by (3). For example, the application of electric fields to alkali chlorides permits a partial separation of electrons and holes in the wake of incident x rays or alpha particles. Of particular interest to us here is the fact that the magnitude of the effective electron-hole coupling is found to be much stronger in the case of a highly ionizing particle. The experiments of Harten and Witt³⁵ on alkali chlorides reveal an order of magnitude greater effective coupling in the case of alpha-particle bombardment compared with x-ray irradiation. Various studies of the motion of electrons and holes in alkali halides indicate that the electron mobility is small, of order $10 \text{ cm}^2/\text{volt sec}$ at room temperature; the hole mobility is estimated to be yet smaller by an order of magnitude.³⁵ Further, the failure to observe internal photoconductivity in pure alkali halides is consistent with the observation of low mobilities and very short displacement lengths for either electrons or holes.³⁶ The over-all situation in the alkali halides is thus one in which electrons and holes are very closely coupled, and the net displacement is small, with the holes remaining relatively more fixed than electrons.

In view of the above, we have chosen in this work to take as our model item (3). On this basis, the incoming particle loses its energy in the formation of electrons and holes, a fraction of which recombine promptly to form excitons; the excitons then diffuse from a line source as monoenergetic particles, suffering capture either at TI^+ sites or at other unspecified traps; capture of an exciton at a TI^+ site results in an excited state which may then decay by emission of a photon or by a nonradiative transition.

We turn now to a detailed description of this process, making the following additional assumptions: (a) For a given incident particle, each TI site and each lattice site can capture at most one exciton; (b) the energy loss of the incoming particle goes almost entirely into ionizing events, with an insignificant energy loss to the direct formation of excitons; (c) the creation and migration of delta rays is neglected; (d) the number of ion pairs per unit path length is directly proportional to dE/dx ; (e)

exciton diffusion occurs radially from the path of the particle and may be described in cylindrical geometry, neglecting end effects at the beginning and end of the particle track. The entire process will be treated as occurring in a thin slice of crystal normal to the path of the particle. The differential energy loss in traversing this slice is dE , and the light output dL is taken as proportional to the number of excitons captured by TI^+ sites (neglecting for the moment concentration quenching effects). Diffusion of energy carriers out of the faces of the slice is very nearly balanced by diffusion in from neighboring slices since dE/dx is slowly varying.

We denote by n_e the initial number of free electrons (or holes) released by the charged particle in the slice of crystal, and by n_0 the number of resulting recombined pairs (excitons). A theoretical treatment of the recombination probability as a function of n_e would involve detailed knowledge of the nature of electron and hole traps, the secondary electron spectrum, electron and hole mobilities, structure dielectric constant, etc. An analysis of this process from first principles is not justified for present purposes as the conclusions to be drawn will not depend on the exact nature of the recombination function. Instead, this aspect of the problem is treated by considering that the electron can suffer two events, either recombining with a hole in the wake of the incident particle, or trapping at an unspecified site in the lattice. Per initial electron, the number of trapped electrons is taken to be proportional to the trap density N_t , a constant, and the number of recombined electrons is taken as proportional to n_e . Thus the recombination probability is given by $n_0/n_e = k_r n_e / (k_t N_t + k_r n_e)$, where k_r and k_t are constants. Since n_e is taken to be directly proportional to dE/dx , $n_e = K(dE/dx)$, this equation can be rewritten as

$$\frac{n_0}{n_e} = \frac{\alpha n_e}{1 + \alpha n_e} = \frac{\alpha K(dE/dx)}{1 + \alpha K(dE/dx)} \quad (2)$$

with $k_r/k_t N_t = \alpha$, a recombination coefficient. We note that the function (2) is very similar to that describing columnar recombination in the wake of an ionizing particle in gases.³⁷ In the latter case α contains a constant determined by the electric field and gas pressure.

As indicated previously, both electrons and holes are expected to suffer small displacements from their point of origin, with the holes remaining relatively more fixed. Accordingly, recombination is considered to occur strictly in the wake of the particle, leaving a line distribution of excitons. Clearly this represents an approximation, as the ionizing effect of the incident particle is by no means confined to a line; the approximation is introduced here for reasons of mathematical simplicity in the following discussion. A more complete description of the initial distribution is not warranted. The diffusion

³⁵ Reviewed by F. Seitz, *Revs. Modern Phys.* **26**, 7 (1954).

³⁶ J. W. Taylor and P. L. Hartman, *Phys. Rev.* **113**, 1421 (1959).

³⁷ See D. H. Wilkinson, *Ionization Chambers and Counters* (Cambridge University Press, New York, 1950), p. 53.

of n_0 energy carriers, originating from a line source, is now described by a one-velocity diffusion equation,

$$\frac{1}{v} \frac{\partial n}{\partial t} = D \nabla^2 n - n(N_i \sigma_i + N_a \sigma_a), \quad (3)$$

where n = density of free carriers = $n(r, t)$, v = velocity of carriers = constant (thermal velocity), D = diffusion constant of carriers (dimensions of cm), N_a = density of unoccupied activator sites = $N_a(r, t)$, N_i = density of lattice traps = constant, σ_a = cross section for capture of a carrier at an activator site = constant, and σ_i = cross section for capture of a carrier at a trapping site = constant. It may be noted that N_a is taken as a function of both space and time, thus permitting the depletion of unoccupied activator sites in the case of a high density of excitons. This is described by a depletion equation,

$$\frac{1}{v} \frac{\partial N_a}{\partial t} = -n N_a \sigma_a. \quad (4)$$

The nature of the lattice traps is not specified further, beyond the fact that their concentration is considered to be sufficiently great such that N_i is a constant. If the principal exciton trapping mechanism is that of self-trapping by polarization of the lattice, then N_i is comparable with the density of lattice sites and is $\sim 10^8$ times N_a . Both N_i and N_a are assumed to be uniformly distributed initially; N_a at $t=0$ will be denoted N_a^0 .

It is appropriate at this point to take note of the various factors which influence the scintillation efficiency, dL/dE . In a slice of crystal, dL/dE represents the number of photons emitted per unit energy loss, and can be written as a product of terms:

$$dL/dE = (1/\epsilon)(n_0/n_e) S P_r P_c \quad (\text{photons/ev}). \quad (5)$$

In Eq. (5), ϵ represents the energy loss of the charged particle required to produce an electron-hole pair; (n_0/n_e) is the initial number of excitons per pair and is given as a function of n_e by Eq. (2); S represents the number of activator sites which capture an exciton per initial exciton; P_r is the radiative transition probability of an isolated excited Tl^+ center; P_c is a concentration quenching parameter which represents the probability that the excited center will escape quenching due to the proximity of another activator site. On the basis of the energy required to produce an ion pair in various solids,³⁸ ϵ is estimated to be about 10 ev per ion pair. It will be shown below that both P_r and P_c are numbers of order unity. The principal task of the present work is thus to calculate S as a function of n_e for crystals containing various concentrations of Tl .

IV. SOLUTION TO EQUATIONS

The approach will be to consider first Eqs. (3) and (4) to determine S as a function of n_0 . The relationship

³⁸ K. G. McKay, Phys. Rev. 84, 829 (1951).

between S and n_e can then be easily found through Eq. (2). Equation (4) can be immediately integrated to yield

$$N_a = N_a^0 e^{-\phi}, \quad (6)$$

where ϕ is defined by

$$\phi \equiv \sigma_a v \int_0^t n(r, t) dt. \quad (7)$$

We note that $\phi = \phi(r, t)$. Further, from Eq. (7)

$$\frac{1}{\sigma_a v} \frac{\partial \phi}{\partial t} = \int_0^t \frac{\partial n}{\partial t} dt. \quad (8)$$

Equation (3) can be rewritten as

$$\frac{\partial n}{\partial t} = v D \frac{1}{r} \frac{\partial}{\partial r} \left(r \frac{\partial n}{\partial r} \right) - v \sigma_i N_i n + \frac{\partial N_a}{\partial t}, \quad (9)$$

where ∇^2 has been replaced by the radial dependence only. Equation (9) can now be integrated over time; using Eqs. (6), (7), and (8), and the initial conditions, we obtain

$$\frac{1}{\sigma_a v} \frac{\partial \phi}{\partial t} = \frac{D}{\sigma_a} \frac{1}{r} \frac{\partial}{\partial r} \left(r \frac{\partial \phi}{\partial r} \right) - \frac{\sigma_i}{\sigma_a} N_i \phi - N_a^0 (1 - e^{-\phi}). \quad (10)$$

We seek a solution to Eq. (10) at very large t , when the diffusion process is over and the carriers have been captured at the various sites. We denote ϕ at large t as ϕ_∞ , a function of r only, so that

$$\frac{1}{r} \frac{d}{dr} \left(r \frac{d\phi_\infty}{dr} \right) - \frac{\sigma_i}{D} N_i \phi_\infty - \frac{N_a^0 \sigma_a}{D} (1 - e^{-\phi_\infty}) = 0. \quad (11)$$

We define

$$\rho \equiv (\sigma_i N_i / D)^{1/2} r, \quad (12)$$

and

$$w \equiv \sigma_a N_a^0 / \sigma_i N_i. \quad (13)$$

With these definitions, Eq. (11) becomes

$$\frac{d}{d\rho} \left(\rho \frac{d\phi_\infty}{d\rho} \right) - \rho \phi_\infty - \rho w (1 - e^{-\phi_\infty}) = 0. \quad (14)$$

Now the number of carriers captured per unit volume per unit time at lattice sites is simply $n v \sigma_i N_i$; the total number of captures at lattice sites is the integral of this function over all space and time. By Eqs. (7) and (12), the total number of carriers captured at lattice sites is found to be

$$\frac{2\pi D}{\sigma_a} \int_0^\infty \phi_\infty \rho d\rho. \quad (15)$$

Similarly, the total number of captures at activator

sites is

$$\frac{2\pi D}{\sigma_a} w \int_0^\infty (1 - e^{-\phi_\infty}) \rho d\rho. \quad (16)$$

Multiplying Eq. (14) by $2\pi D/\sigma_a$ and integrating, we obtain

$$\begin{aligned} \frac{2\pi D}{\sigma_a} \int_0^\infty \frac{d}{d\rho} \left(\frac{\rho d\phi_\infty}{d\rho} \right) d\rho &= \frac{2\pi D}{\sigma_a} \int_0^\infty \phi_\infty \rho d\rho \\ &+ \frac{2\pi D}{\sigma_a} w \int_0^\infty (1 - e^{-\phi_\infty}) \rho d\rho. \end{aligned} \quad (17)$$

Reference to Eqs. (15) and (16) shows that the right-hand side of Eq. (17) is the sum of lattice captures plus activator captures, so that the left-hand side is simply the total initial number of carriers, n_0 . The problem is now reduced to one of solving Eq. (14) for ϕ_∞ as a function of ρ , and then evaluating any two of the three integrals in Eq. (17) to obtain the number of captures at activator sites per initial carrier. This gives one value of S for a particular n_0 ; the process must then be repeated for various n_0 to determine S as a function of n_0 .

Reference to Eq. (14) shows that the only constant involved is the parameter w , defined in Eq. (13). It is seen that w is proportional to the initial density of activator sites, hence the Tl concentration; it is through this parameter that the concentration dependence enters the problem. Fortunately, it is possible to obtain an approximate numerical value for w by reference to experiments in which the scintillation response of NaI(Tl) to gamma rays has been measured as a function of Tl concentration.³⁹ A theoretical expression for the relative luminescence efficiency as a function of activator concentration has been given by Johnson and Williams⁴⁰; for present purposes this relationship may be written

$$dL/dE \propto \frac{c(1-c)^z}{c + (\sigma_l/\sigma_a)(1-c)}, \quad (18)$$

where c is the mole fraction of the activator and z is an effective number of lattice sites surrounding a given activator such that concentration quenching will occur if another activator atom is contained within z . The experimental data³⁹ on intensity versus concentration have been determined for gamma rays of energy 0.662 Mev. In this case the observed pulse height versus energy relationship is very nearly linear and nearly passes through the origin, so that to a good approximation $L/E \approx dL/dE$; it is thus appropriate to apply Eq. (18) to the experimental pulse height versus concentration curve to obtain values of σ_l/σ_a and z . In so doing,

³⁹ J. A. Harshaw, H. C. Kremers, E. C. Stewart, E. K. Warburton, and J. O. Hay, U. S. Atomic Energy Commission Report NYO-1577, 1952 (unpublished).

⁴⁰ P. D. Johnson and F. E. Williams, J. Chem. Phys. **18**, 1477 (1950).

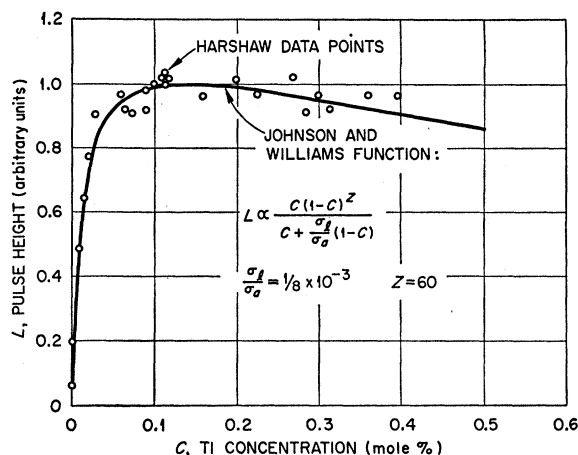


Fig. 4. Pulse height as a function of Tl concentration for NaI(Tl) crystals. Experimental data from reference 39. Smooth curve is a fit of the Johnson-Williams function to experiment using parameters shown.

it is necessary to use the known energy conversion efficiency of NaI(Tl)⁴¹ and to use a numerical value of n_0/n_e which is derived later. A rather good fit to the data of Harshaw *et al.*³⁹ can be obtained with $\sigma_a/\sigma_l = 8 \times 10^3$ and $z = 60$ (see Fig. 4). If we associate our N_l with the density of lattice sites, then $c = N_a/N_l$ and $w = c\sigma_a/\sigma_l$. Thus, for a typical commercial NaI(Tl) crystal of activator concentration 1×10^{-3} , w is approximately 8. This value of w is subject to considerable uncertainty by the nature of its derivation, but is expected to be of the right order. Fortunately, the results to be obtained are rather insensitive to the absolute value of w . We note here that Eq. (18) can be written

$$dL/dE \propto \left(\frac{w}{1+w} \right) (1-c)^z, \quad (19)$$

where $(1-c)$ in the denominator of Eq. (18) is taken as unity since c is of order 10^{-3} . It will be seen later that the term $w/(1+w)$ is contained within the function S , so that we may associate the concentration quenching term $(1-c)^z$ with P_e of Eq. (5). Since c is small, P_e differs from unity by only a few percent. Finally, knowledge of the energy conversion efficiency and the factors entering Eq. (5) permits the assignment of a lower limit to P_r of about 0.6. The upper limit is of course unity. In the evaluation of w we have taken a compromise value of $P_r = 0.8$.

We return now to the central problem of solving Eq. (14) for ϕ_∞ as a function of ρ . As it stands, Eq. (14) is not amenable to direct analytical solution. A simple solution is made possible, however, if we approximate the function $(1 - e^{-\phi_\infty})$ by three appropriately chosen straight-line segments. If we denote the three straight-

⁴¹ W. J. Van Sciver and L. Bogart, IRE Trans. on Nuclear Sci. NS-5, 90 (1958).

line segments by y_i as a function of ϕ_∞ , then we choose

$$\begin{aligned} y_1 &= \phi_\infty & \text{for } 0 \leq \phi_\infty < 0.5, \\ y_2 &= (1/6)\phi_\infty + 5/12 & \text{for } 0.5 \leq \phi_\infty < 3.5, \\ y_3 &= 1 & \text{for } 3.5 \leq \phi_\infty. \end{aligned} \quad (20)$$

Thus ϕ_∞ is divided into three regions. In any one of these regions the solution to the modified Eq. (14) is now given by

$$\phi_{\infty,i} = A_i I_0[\rho(1+m_i w)^{1/2}] + B_i K_0[\rho(1+m_i w)^{1/2}] - w b_i / (1+m_i w), \quad (21)$$

where $i=1, 2, 3$, and where m_i and b_i are the slope and intercept of the straight-line approximation to the exponential term. The solutions I_0 and K_0 are modified Bessel functions of the first and second kind. The coefficients A_i and B_i may be obtained from the requirement that both ϕ_∞ and its first derivative be continuous in going from one region to another. By this means, it is possible to obtain a solution to Eq. (14) to determine S , the number of excitons captured at Tl sites per initial exciton, as a function of the initial number of excitons. A plot of this function for the cases $w=8$ and 0.8 is given in Fig. 5, where the abscissa represents the integral from the left-hand side of (17), and is thus $n_0 \sigma_a / 2\pi D$. It is seen in Fig. 5 that the function approaches $w/(1+w)$ at low n_0 . This is exactly the behavior expected: For very low ionization densities the fraction of excitons captured by activator sites should be just $N_a^0 \sigma_a / (N_a^0 \sigma_a + N_l \sigma_l)$, which is the same as $w/(1+w)$. For larger values of n_0 the function S decreases as a result of the depletion of unoccupied activator sites.

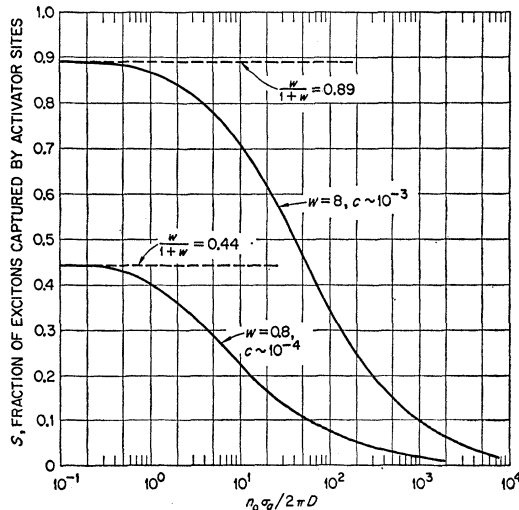


FIG. 5. Calculated fraction of energy carriers captured on activator sites as a function of $n_0 \sigma_a / 2\pi D$. Upper curve for $w=8$ corresponds to activator concentration of about 1×10^{-3} . Lower curve for $w=0.8$ corresponds to activator concentration of about 1×10^{-4} . Both curves are obtained from the solution of Eqs. (3) and (4). Comparison of the upper curve with experimental data for high- dE/dx particles leads to a numerical value for $\sigma_a / 2\pi D$, as discussed in text.

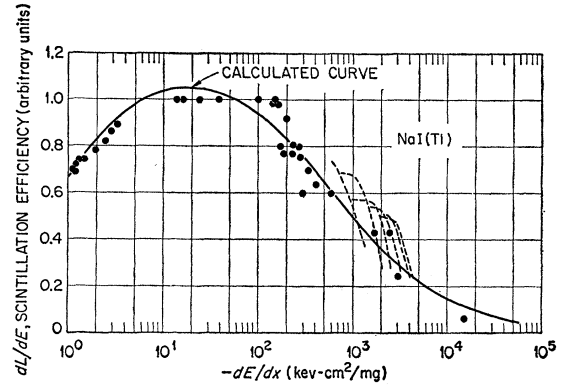


FIG. 6. Calculated scintillation efficiency versus dE/dx superimposed on experimental data. The normalization and choice of $\alpha K = 2(\text{kev-cm}^2/\text{mg})^{-1}$ are chosen to give a best fit with experiment.

As a check on the accuracy of the approximation to the exponential term of (14), a different set of straight lines was chosen so as to overestimate the exponential growth function for ϕ_∞ in the intermediate region (corresponding to y_2), whereas the lines given by Eqs. (20) provide an underestimate. The difference in the calculated values of S using the two approximations was very small, the maximum deviation amounting to less than 3% for the region where S is near half-maximum. It is concluded that the straight-line approximation is quite adequate for present purposes.

The remaining task is now to multiply the ordinate of Fig. 5 by n_0/n_e , and the abscissa by n_e/n_0 , to obtain the number of excited Tl sites per initial electron-hole pair versus $n_e \sigma_a / 2\pi D$. The recombination parameter αK in Eq. (2) must be determined by a best fit to the experimental data of either Fig. 2 or Fig. 3. The final calculated curve is shown in Fig. 6, superimposed on the various data points taken from Fig. 2. The calculated curve is based on a choice of $\alpha K = 2(\text{kev-cm}^2/\text{mg})^{-1}$ and a normalization chosen to give a best fit to experiment. Comparison of the calculated curve with experiment also establishes the numerical relationship between differential energy loss and the abscissa of the theoretical curve which is $n_e \sigma_a / 2\pi D$. This numerical relationship, along with the estimated value of $\epsilon = 10$ ev/pair, determines the constant $2\pi D / \sigma_a$, which is found to be $5 \times 10^6 \text{ cm}^{-1}$ for NaI(Tl).

V. RESULTS OF SOLUTION AND CONSEQUENCES

The calculated curve of Fig. 6 is seen to provide a reasonable fit to the over-all trend of the experimental data. The most significant departure of the calculated curve from experiment is in the case of the heavy particles, where the experimental data fall much more steeply and indicate a different curve for each particle. As indicated previously, this type of behavior cannot be interpreted within the framework of the model adopted here. A more complete treatment of the present subject would have to include a detailed examination of the

charged particle interactions in the crystal. In particular, attention should be given to the energy lost to delta rays as these constitute secondary particles capable of stimulating luminescence radiation with a high scintillation efficiency.

The behavior of the calculated scintillation efficiency curve of Fig. 6 is the consequence of two processes. The falling characteristic for large dE/dx is due to the depletion of unoccupied activator sites. The initial rise of the scintillation efficiency for low dE/dx (characteristic of electrons) is brought about by the recombination process. It may be particularly noted that the recombination function (2) does not contain the Tl concentration. Thus, on the basis of the present model, the *nonlinear response of NaI(Tl) to electrons arises as an intrinsic property of the crystal, and would be unaffected by changes in activator concentration.* On the other hand, if the scintillation process were described by the binary diffusion of electrons and holes followed by recombination at Tl sites, then the recombination probability would depend on the density of activator sites and the shape of the electron response curve should be a function of Tl concentration. For this reason it would be of interest to examine the electron response of alkali iodide scintillators containing varying amounts of activator.

The theoretical curve of Fig. 6 has been derived with particular reference to NaI(Tl). By virtue of the close similarity in experimental data from NaI(Tl) and CsI(Tl), Figs. 2 and 3, the calculated curve can also be applied to the CsI(Tl) data. A more direct comparison of the theoretical results with experiment can be made by calculating the pulse height versus energy for various particles using the curve of Fig. 6. As an example, the calculated pulse-height response curves for protons, alphas, and C^{12} ions are shown in Fig. 7, along with the experimental data for these particles on CsI(Tl).²² The calculation has been normalized to the experimental data for alpha particles between 1 and 2 Mev; having chosen this one normalization, the shape and position of each of the calculated curves of Fig. 7 is

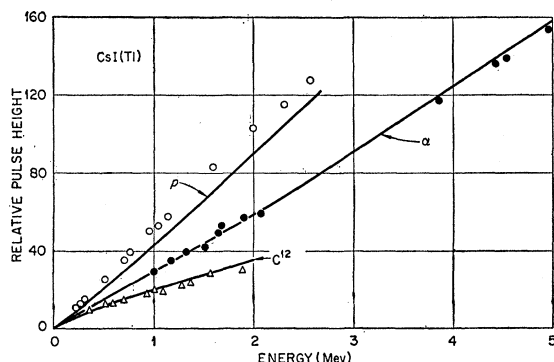


FIG. 7. Calculated pulse height versus energy for p , α , and C^{12} in CsI(Tl), superimposed on experimental data from reference 22. Calculated curves are based on smooth curve of Fig. 6 and are normalized to experimental points for alphas between 1 and 2 Mev.

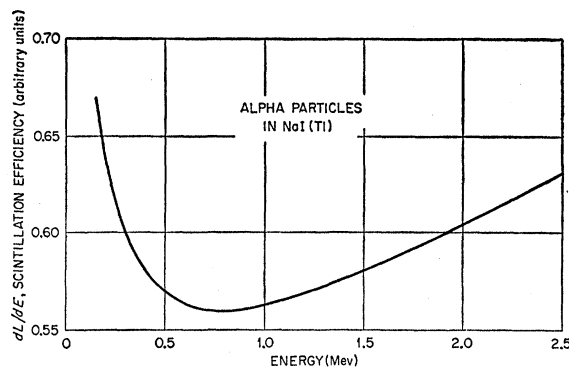


FIG. 8. Scintillation efficiency as a function of energy for alpha particles in NaI(Tl), calculated from Figs. 1 and 6. Note expanded scale on ordinate.

uniquely fixed. It is seen that the agreement with experiment is good for alphas and C^{12} ions, but the calculated proton curve is some 10 to 15% lower than the experimental points. This is a consequence of the fact that the theoretical curve of Fig. 6 does not fall as steeply as the experimental data.

One feature of the calculated pulse height versus energy curve which may be noted here arises from the fact that the differential energy loss of a charged particle passes through a maximum. Reference to Fig. 1 shows that this maximum occurs just below 1 Mev for alpha particles and below 0.1 Mev for protons. As a consequence of this, a plot of dL/dE versus energy passes through a minimum at that energy where dE/dx is a maximum. As an example, Fig. 8 illustrates the behavior of dL/dE versus energy for an alpha particle in NaI(Tl), calculated on the basis of Figs. 1 and 6. The ordinate of Fig. 8 is the same as that of Fig. 6. The behavior of dL/dE as shown in Fig. 8 thus predicts a kink in the pulse height versus energy curve: for energies below ~ 1 Mev, the pulse-height curve has a decreasing slope and bends toward the energy axis, whereas for higher energies it bends away. There is considerable experimental evidence in the higher energy region illustrating the increasing slope. There have been fewer experimental studies in the region below 1 Mev; however, the data of Allison and Casson¹⁶ on alpha particles in NaI(Tl) up to 0.3 Mev indicate a distinctly decreasing slope with increasing energy, in qualitative agreement with the prediction of Fig. 8. It would be of interest to examine carefully the pulse height versus energy relationship for alpha particles on, say, NaI(Tl) or CsI(Tl) in the region of 1 Mev to test the predicted behavior.

We turn next to an estimate of the diffusion length of the energy carriers. The diffusion length L is given by

$$L^2 = D / (N_a \sigma_a + N_l \sigma_l). \quad (22)$$

Also, in cylindrical geometry the mean square distance before capture is related to the diffusion length by $\langle r^2 \rangle = 4L^2$. It should be noted that in the present work L in general is not a constant since N_a is not a constant.

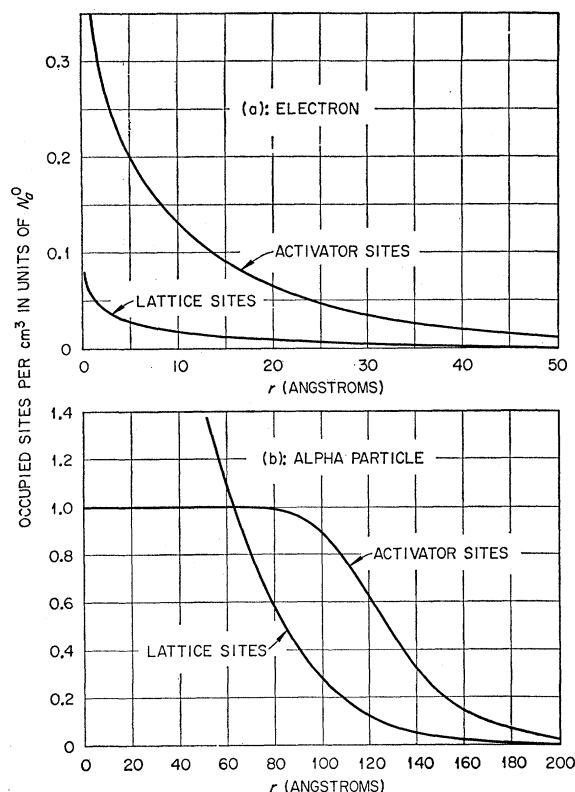


FIG. 9. Distribution of energy carriers on activator sites and trapping sites after the diffusion and capture processes are complete. (a) Low- dE/dx case corresponding to incident electron of 0.15 Mev. (b) High- dE/dx case corresponding to 4-Mev alpha. Note different scales in (a) and (b). Curves apply to NaI(Tl) of activator concentration $\sim 1 \times 10^{-3}$.

If the discussion of diffusion length is limited to the case of low ionization densities, then the saturation mechanism is negligible and N_a is nearly constant, equal to N_a^0 . The following discussion thus applies to low- dE/dx events, e.g., electrons. For a NaI(Tl) crystal of 0.1% activator concentration, it was previously found that $\sigma_a N_a^0 / \sigma_t N_t \approx 8$. Equation (22) then becomes $L^2 = 0.88 D / N_a^0 \sigma_a$. Also, it was found previously that $D / \sigma_a = (1/2\pi)(5 \times 10^6) \text{ cm}^{-1}$. The density of Tl sites is $1.5 \times 10^{19} \text{ per cm}^3$, so that L is calculated to be about 20 Å and the root mean square distance before capture is about 40 Å. This value of diffusion length is at best a rough value, particularly since it depends on previously estimated quantities such as ϵ and w . It should be significant, however, as to order of magnitude; in particular, the diffusion length found here is quite small and indicates that the energy transport occurs in a very limited region. Theoretical estimates of the "migration length" of an exciton in an idealized ionic crystal generally indicate an upper limit of order 10^4 Å. The presence of impurity centers, however, is expected to reduce the exciton lifetime, hence diffusion length; calculations indicate³⁵ that an impurity concentration of order 10^{15} per cm^3 might reduce the exciton lifetime by an order

of magnitude. In the present case we are dealing with impurity concentrations of order 10^{19} per cm^3 , so that the small value of diffusion length derived here does not seem unrealistic.

It is instructive to plot the distribution of excitons captured on Tl sites and on lattice sites for the case of both a low- dE/dx and a high- dE/dx particle. According to the earlier discussion, the distribution of excited Tl centers (i.e., number of Tl sites per cm^3 which have captured an exciton) is given by the function $N_a^0 w \{1 - \exp[-\phi_\infty(r)]\}$, while the density of excitons captured on lattice sites is simply $N_a^0 \phi_\infty(r)$. The function $\phi_\infty(r)$ is available from the previous solution to (14); the constant relating ρ to r in Eq. (12) can be determined numerically from the preceding discussion, with the result $r = \rho \times 67 \text{ Å}$. Both distribution functions are plotted in Fig. 9 for the case of a 0.15-Mev electron ($dE/dx = 2 \text{ kev-cm}^2/\text{mg}$) and a 4-Mev alpha particle ($dE/dx = 400 \text{ kev-cm}^2/\text{mg}$). In Fig. 9(a), the low- dE/dx case, it is seen that both curves have nearly the same functional dependence and are separated in magnitude by a factor of $w = 8$. This is the "no-saturation" case, in which the ratio of excitons captured by Tl sites and by lattice sites is just the ratio of the densities of sites weighted by their capture cross sections. The behavior shown in Fig. 9(b), the high- dE/dx case, is significantly different. The density of activated Tl sites for small r is a constant equal to the initial density of Tl ions, so that all possible activator sites have been filled; in the same region, the density of excitons captured on lattice sites is very large. Thus, the filling of all available activator sites at small r forces the capture of many excitons by lattice traps. At large r , the density of excitons is at all times small, and the distribution functions again differ only by the constant factor w . Thus, the decreasing scintillation efficiency for high- dE/dx particles is due to two factors: (a) the competition between activator sites and lattice traps for capture of the energy carriers, and (b) the fact that the *density of activator sites is much less than the density of traps*. On the other hand, if the density of traps were less than the density of activators then it would be the traps which were depleted and the scintillation efficiency would actually increase with dE/dx . Clearly, if there were no traps at all the distribution would simply move out to larger r until every carrier occupied an activator and the scintillation efficiency would be constant in dE/dx .

The distribution function for excited activators can be multiplied by rdr and integrated to obtain the number of excited Tl sites within a cylinder of radius r . The result of doing this for the two cases of Fig. 9 shows that 95% of the excited Tl sites are contained within a radius of $\sim 90 \text{ Å}$ for the electron case, and within $\sim 170 \text{ Å}$ for the alpha particle. This difference illustrates the fact that the carrier distribution is pushed out to larger radii for high- dE/dx events. It should be understood in this discussion that no account is taken of the formation of

delta rays, so that the above distributions apply only to excitons formed in the wake of the primary particle. The migration of delta rays from the path of the incident particle will have the effect of increasing the apparent volume from which light is emitted. It is appropriate to note the experimental work of Zavoiskii and Smolkin³¹ who measured an upper limit on the diameter of the light-emitting column in the case of 5.3-Mev alphas on CsI(Tl). Their experiment, which was limited by the resolution of the optical apparatus, indicated a maximum width of 1 micron. The estimated diameter of several hundred angstroms based on Fig. 9 is thus not inconsistent with experiment.

In view of the above calculations of the carrier distribution function, we may return to examine the initial assumption of cylindrical symmetry with neglect of end effects. This assumption seems to be quite good for protons, alphas, or heavier ions in the energy regions involved here (including fission fragments) as the range of these particles in an alkali iodide is of the order of 10^{-4} or 10^{-3} cm, whereas the column containing the distributed excitons is seen to have a diameter of order hundreds of angstroms. Thus, the ratio of length to diameter of the column is large and cylindrical symmetry is appropriate. A somewhat anomalous situation arises, however, for very low dE/dx particles such as electrons. In this case, where dE/dx is of order 1 to 10 kev-cm²/mg, a pair will be formed on the average at distances of about 250 to 25 Å along the path of the primary particle and these distances are comparable with or greater than the exciton diffusion distances. In this case, a more appropriate geometry probably would be that of a series of point sources. Fortunately, in this low- dE/dx region, the results of the calculation should be rather insensitive to the geometry and need not be modified for present purposes. The reason is simply that there is virtually no saturation of Tl centers for these values of dE/dx and the excitons will be distributed on Tl sites and trapping sites in the ratio w , independent of the source geometry. In the region of $dE/dx = 50$ kev-cm²/mg and above, where saturation effects begin to be significant, pairs will be formed only a few angstroms apart and cylindrical geometry is appropriate. It should be further noted that throughout the calculation we have approximated a discrete lattice as a continuous medium.

VI. CONCENTRATION-DEPENDENT AND TEMPERATURE-DEPENDENT EFFECTS

We turn next to a study of the effect of activator concentration on the behavior of the scintillation efficiency curve. A new solution to the equations corresponding to a different Tl concentration is obtained by picking a new value of w in Eq. (14) and repeating the process to obtain dL/dE as a function of dE/dx . A family of curves is obtained by this method, as shown in Fig. 10. The activator concentration c associated with

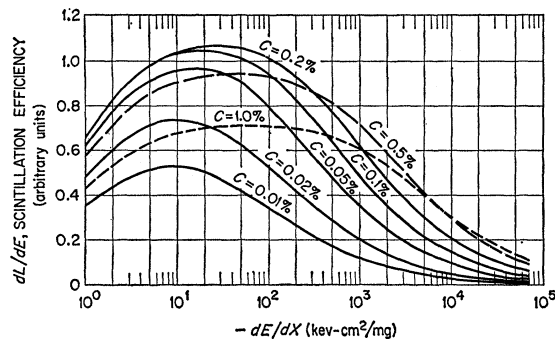


FIG. 10. Calculated scintillation efficiency as a function of dE/dx for crystals of different Tl concentration.

each curve is derived from the relationship

$$w = (\sigma_a N_a^0 / \sigma_l N_l) = (8 \times 10^3)c, \quad (23)$$

where the ratio σ_a/σ_l was previously determined as 8×10^3 , and where N_l is associated with the density of lattice sites so that $N_a^0/N_l = c$. This latter association is of course an assumption, so that the absolute value of concentration associated with any curve of Fig. 10 is uncertain; the significant feature is thus the relative concentration in going from one curve to another.

Several points may be noted in connection with Fig. 10. First, it is seen that the difference in scintillation efficiency between, say, protons and heavy ions ($dE/dx = 50$ and 500 kev-cm²/mg) is minimized for high concentrations and is a maximum for a low-concentration crystal. This behavior is of course due to the fact that the saturation effect is less pronounced in a crystal with a higher density of activator sites. Particular attention may be directed to the $c = 1.0\%$ curve which is quite flat over a wide range of dE/dx . In such a crystal, the response to protons and alphas would be nearly the same.

A second point of interest has to do with the scintillation efficiency as a function of concentration for a fixed dE/dx . It is seen in Fig. 10 that for the lowest dE/dx the scintillation efficiency initially increases with concentration and passes through a maximum, in agreement with the behavior of Fig. 4. In contrast with this, the scintillation efficiency for highest dE/dx is seen to be a monotonically increasing function of concentration up to 1.0% . The shape of the scintillation efficiency versus concentration curve thus depends on dE/dx in a manner which can be obtained from Fig. 10. The experimental data of Eby and Jentschke⁸ on NaI(Tl) crystals with varying Tl concentration permit a comparison of the predictions of Fig. 10 with experiment. The experimental data are available as pulse height versus concentration for 5.3-Mev alphas, 11.5-Mev deuterons, and 23-Mev alphas. In order to make the comparison, the scintillation efficiency for a particular concentration crystal from Fig. 10 was integrated over energy to obtain the pulse height L for each of the three particles used in the experiment. The comparison is shown in

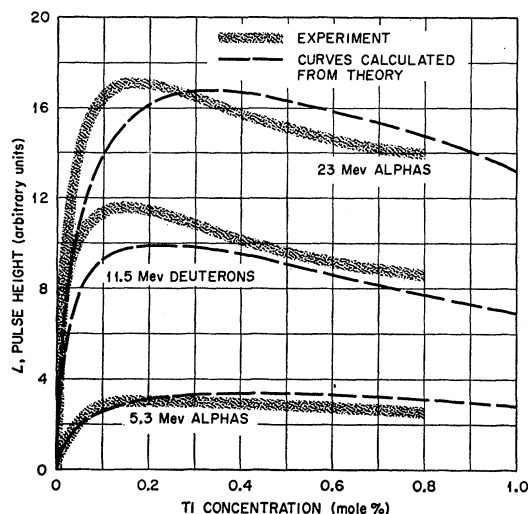


FIG. 11. Pulse height versus Tl concentration for different particles on NaI(Tl). Experimental curves from Eby and Jentschke, reference 8. Calculated curves result from integration of curves in Fig. 10, and are normalized to experiment with the choice of one constant.

Fig. 11; by virtue of the arbitrary ordinate, the calculated data have been normalized to experiment with the choice of one normalizing constant. It is seen that the agreement with experiment is reasonably good, both as to the relative magnitudes of the curves and as to their shapes. It may be further noted that the maxima in the calculated curves occur at a concentration which is within a factor of 2 agreement with the experimental curves, thus lending support to the validity of Eq. (23) and the assumption that $N_a^0/N_t = c$. It would be of interest to examine the scintillation efficiency as a function of Tl concentration for very high dE/dx particles, as Fig. 10 indicates a monotonically increasing function in the concentration range studied here.

We turn finally to temperature-dependent behavior. In activated alkali iodides, the dependence of light intensity on temperature is usually described⁴² in terms of the temperature dependence of the radiative transition probability. In connection with the present work, we note additional effects which might contribute to a temperature dependence. Tomura⁴³ has suggested that the cross section for excitation of the Tl^+ ion by a moving exciton, σ_a , is expected to be a function of temperature. If one does not consider the diffusion aspects of the

problem, Tomura shows that the relative luminescent intensity should be proportional to $[a + b \exp(-E/kT)]^{-1}$, where a and b are constants and E is the energy difference between the states of the mobile exciton and the trapped exciton. This temperature dependence is functionally the same as that predicted by the conventional description mentioned earlier.⁴² In terms of the present work, however, a temperature dependence of σ_a leads to a temperature dependence of w , Eq. (13), and a change in w is equivalent to a change in the activator concentration. Thus, the present model predicts a change in *shape* of the dL/dE versus dE/dx curve with temperature. If the activation energy E is positive, as expected, then σ_a increases with decreasing temperature and the dL/dE versus dE/dx curve at low temperatures should correspond more nearly to that of a crystal with higher activator concentration. A change in temperature is not identically equivalent to a change in concentration, however, as other parameters in the present model may be temperature dependent, e.g., the recombination probability n_0/n_e , the diffusion constant D , or the radiative transition probability P_r . The principal point is the following: If the usual interpretation of the temperature dependence is correct and arises only from the radiative transition probability then the scintillation efficiency curve should change only in magnitude as a function of temperature, but not in shape. If the dependence of σ_a on temperature as suggested by Tomura is a significant effect, then the shape of the curve should be a function of temperature. It would be of considerable interest to obtain experimental data on the dL/dE versus dE/dx curve for, say, NaI(Tl) at liquid nitrogen temperature to test this prediction. We may note one set of experiments⁴⁴ on europium-activated LiI which confirms a change in the shape of the curve in going from room temperature to liquid nitrogen temperature. The experimental data are consistent with a flatter dL/dE versus dE/dx curve at low temperatures, analogous to a higher concentration crystal.

ACKNOWLEDGMENTS

The authors wish to acknowledge very helpful discussions with several colleagues, including E. G. Harris, J. H. Barrett, and H. C. Schweinler of this Laboratory, and F. E. Williams of the General Electric Research Laboratory. We are especially indebted to the late A. Schopf of this Laboratory for indicating the method of solution to the equations. R. W. Peelle kindly reviewed the manuscript.

⁴² See, for example, J. Bonanomi and J. Rossel, *Helv. Phys. Acta* **25**, 725 (1952).

⁴³ M. Tomura, *J. Phys. Soc. Japan* **15**, 1508 (1960).

⁴⁴ R. B. Murray, *Nuclear Instr.* **2**, 237 (1958).